Polyhedron 28 (2009) 1822–1825

Contents lists available at ScienceDirect

Polyhedron

journal homepage: www.elsevier.com/locate/poly

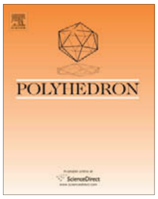

Study on the valence fluctuation and the magnetism of an iron mixed-valence complex, $(n\text{-}C_4H_9)_4N[Fe^{II}Fe^{III}(mto)_3](mto = C_2O_3S)$

Koichi Kagesawa, Yuki Ono, Masaya Enomoto, Norimichi Kojima *

Graduate School of Arts and Science, The University of Tokyo, 3-8-1 Komaba, Meguro-ku, Tokyo 153-8902, Japan

ARTICLE INFO

Article history:
Available online 2 March 2009

Keywords:
Iron mixed-valence complex
Valence fluctuation

ABSTRACT

In the case of iron mixed-valence complexes whose spin states are situated in the spin-crossover region, conjugated phenomena coupled with spin and charge are expected. In general, the Fe site coordinated by six S atoms is in the low-spin state, while the Fe site coordinated by six O atoms is in the high-spin state. From this viewpoint, we have synthesized and investigated physical properties for an monothiooxalato-bridged (mto = C_2O_3S) iron mixed-valence complex, $(n\text{-}C_4H_9)_4N[Fe^{II}Fe^{III}(mto)_3]$, consisting of $Fe^{III}O_3S_3$ and $Fe^{II}O_6$ octahedra, which behaves as a ferrimagnet with its magnetic transition temperature of $T_N = 38$ K and Weiss temperature of $\theta = -93$ K. From the analysis of ^{57}Fe Mössbauer spectra of ^{57}Fe enriched complexes, $(n\text{-}C_4H_9)_4N[^{57}Fe^{II}Fe^{III}(mto)_3]$ and $(n\text{-}C_4H_9)_4N[Fe^{II57}Fe^{III}(mto)_3]$, the charge transfer between Fe^{II} and Fe^{III} exists in the paramagnetic phase. Considering the time window of ^{57}Fe Mössbauer spectroscopy, the time scale of the valence fluctuation is at least slower than 10^{-7} s. In order to confirm the valence fluctuation between Fe^{II} and Fe^{III}, we investigated the dielectric constant and found an anomalous enhancement attributed to the Fe valence fluctuation between 170 and 250 K.

1. Introduction

One of the most important topics in recent research in the field of molecular solids is to produce various kinds of multifunctionalities coupled with transport, optical or magnetic properties [1–3]. Recently, Kojima, et al. discovered a new type of phase transition for a dithiooxalato-bridged iron mixed-valence complex $(n\text{-}C_3H_7)_4N[Fe^{II}Fe^{III}(dto)_3]$ (dto = $C_2O_2S_2$), where the thermally induced charge transfer phase transition reversibly occurs around 120 K in order to minimize the free energy in the whole system [4]. $(n\text{-}C_3H_7)_4N[Fe^{II}Fe^{III}(dto)_3]$ has a two-dimensional honeycomb network structure with an alternating array of Fe^{II} and Fe^{III} atoms through dto ligand and the $(n\text{-}C_3H_7)_4N^+$ cation layers are intercalated between two $[Fe^{II}Fe^{III}(dto)_3]_\infty$ layers [5]. In the high temperature phase (HTP), the Fe^{III} ($S = 1/2$) and Fe^{II} ($S = 2$) sites are coordinated by six S atoms and six O atoms, respectively. In the low temperature phase (LTP), on the other hand, the Fe^{III} ($S = 5/2$) and Fe^{II} ($S = 0$) sites are coordinated by six O atoms and six S atoms, respectively. Moreover, $(n\text{-}C_3H_7)_4N[Fe^{II}Fe^{III}(dto)_3]$ behaves as a ferromagnet with $T_C = 7$ K.

Here, we focus on a new mixed-valence complex, $(n\text{-}C_4H_9)_4N[Fe^{II}Fe^{III}(mto)_3]$ (**1**) [6]. This complex consisting of $Fe^{III}O_3S_3$ and $Fe^{II}O_6$ octahedra has a possibility of dielectric response and nonlinear optical effect caused by the lack of inversion symmetry at the Fe^{III} site. Moreover, it should be noted that the Fe site coordinated by three S atoms and three O atoms such as the Fe sites in tris(monothio carbamato)iron(III) complexes are situated in the spin-crossover region [7]. In contrast to a lot of oxalato-bridged complexes, a few monothiooxalato-bridged complexes are known [8,9].

In this paper, we employed ^{57}Fe enriched samples in which Fe^{II} or Fe^{III} was substituted with ^{57}Fe, $(n\text{-}C_4H_9)_4N[^{57}Fe^{II}Fe^{III}(mto)_3]$ (**2**) and $(n\text{-}C_4H_9)_4N[Fe^{II57}Fe^{III}(mto)_3]$ (**3**), to investigate the magnetic properties and the Fe valence states of **1** by means of magnetic susceptibility measurement and ^{57}Fe Mössbauer spectroscopy. Moreover, we investigated the temperature dependence of the dielectric constant and found an anomalous enhancement caused by the Fe valence fluctuation in a wide temperature range.

2. Experimental

2.1. Preparation of $(n\text{-}C_4H_9)_4N[Fe^{II}Fe^{III}(mto)_3]$

2.1.1. Preparation of $K_2(mto)$

Oxalyl-diethyl (4.38 g, 30 mmol) and KHS (2.17 g, 30 mmol) were dissolved in ethanol of 35 ml, then the solution was refluxed for 24 h. The solvent was removed by evaporation. The yellow precipitate was washed with ether and dissolved in fresh ethanol of 40 ml. To this, a solution of potassium hydroxide (1.68 g, 30 mmol) in ethanol (10 ml) was added dropwise and the solution was

---

* Corresponding author. Tel./fax: +81 3 5454 6741.
E-mail address: cnori@mail.ecc.u-tokyo.ac.jp (N. Kojima).

0277-5387/$ - see front matter © 2009 Elsevier Ltd. All rights reserved.
doi:10.1016/j.poly.2009.01.011

allowed to stir for an additional 15 min while a milky suspension developed. After cooling the solution at 0 °C (ice bath), K_2(mto) was isolated by suction filtration and washed several times with ether.

*2.1.2. Preparation of (n-C_4H_9)$_4$N[$Fe^{II}Fe^{III}$(mto)$_3$] (**1**)*

In the formation process of **1**, according to HSAB principle (Hard and Soft Acids and Bases principle), the flipping of mto by 180° would take place here and there, which induces a linkage-isomerization from –Fe^{III}–SOC_2O_2–Fe^{II}– to –Fe^{III}–O_2C_2OS–Fe^{II}– [10]. In order to restrain the linkage-isomerization, **1** was synthesized at −20 °C. A methanol solution of iron(III) nitrate (0.14 g, 0.35 mmol) was added to a methanol solution of K_2(mto) (0.19 g, 1.05 mmol). After stirring for 5 min, [Fe^{III}(mto)$_3$]$^{3-}$ solution was given. This solution was filtered once to remove solid impurities. The filtrate was cooled at −20 °C, and was added a methanol solution (20 ml) of iron(II) chloride (68.9 mg, 0.35 mmol), (*n*-C_4H_9)$_4$NBr(112.8 mg, 0.35 mmol) and ascorbic acid (17.6 mg, 0.1 mmol). The mixture was stirred for 3 h. The dark-brown product was collected by suction filtration and dried in vacuo. Elemental *Anal.* Calc. for $C_{22}H_{36}NO_9S_3Fe_2$: C, 39.65; H, 5.45; N, 2.1. Found: C, 38.79; H, 5.50; N, 2.01%.

*2.1.3. Preparation of (n-C_4H_9)$_4$N[$^{57}Fe^{II}Fe^{III}$(mto)$_3$] (**2**)*

(*n*-C_4H_9)$_4$N[$^{57}Fe^{II}Fe^{III}$(mto)$_3$] was prepared in a similar way to Section 2.1.2. In this process, $^{57}FeCl_2 \cdot 4H_2O$ used as Fe^{II} source was prepared by dropping hydrochloric acid to powdered ^{57}Fe under N_2. Elemental *Anal.* Calc. for $C_{22}H_{36}NO_9S_3Fe_2$: C, 39.65; H, 5.45; N, 2.1. Found: C, 39.49; H, 5.65; N, 2.03%.

*2.1.4. Preparation of (n-C_4H_9)$_4$N[$Fe^{II57}Fe^{III}$(mto)$_3$] (**3**)*

(*n*-C_4H_9)$_4$N[$Fe^{II57}Fe^{III}$(mto)$_3$] was prepared in a similar way to Section 2.1.2. In this process, $^{57}Fe(NO_3)_3 \cdot 9H_2O$ used as Fe^{III} source was prepared by dropping nitric acid to powdered ^{57}Fe under N_2. Elemental *Anal.* Calc. for $C_{22}H_{36}NO_9S_3Fe_2$: C, 39.65; H, 5.45; N, 2.1. Found: C, 38.71; H, 5.51; N, 2.11%.

2.2. Measurements

The static magnetic susceptibility was measured by a Quantum Design, MPMS5 SQUID susceptometer under 5000 Oe between 2 and 300 K. The zero field cooled magnetization (ZFCM) and field cooled magnetization (FCM) were also measured for investigating the ferrimagnetic phase in the temperature range of 2–45 K under 30 Oe. The remnant magnetization (RM) was measured in the same temperature region under zero field. A sample was wrapped in polyethylene film and mounted inside the straw. The magnetic susceptibility obtained was corrected for the background and the core diamagnetism estimated from Pascal's constants.

The ^{57}Fe Mössbauer spectra were measured for **2** and **3**. The spectra were calibrated by using the six lines of a body-centered cubic iron foil (α-Fe), the center of which was taken as zero isomer shift. The ^{57}Fe Mössbauer spectra at low temperature were performed with a closed-cycle helium refrigerator cryostat (Iwatani Co., Ltd.).

The dielectric constant measurements were carried out between 4.2 and 300 K by an Agilent, 4284A LCR Meter with alternating electric fields of 1, 10 and 100 kHz. Polar plates were formed by carbon pastes and gold wires were fixed on the both faces of the pellet sample.

3. Results and discussion

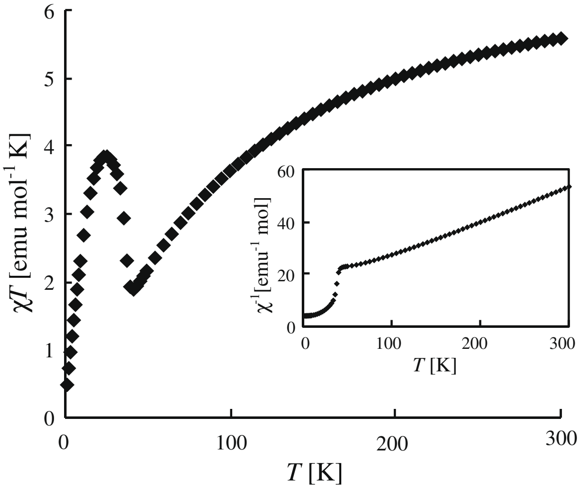

Fig. 1. Temperature dependence of the effective magnetic moment for **1**. Inset is temperature dependence of the inverse magnetic susceptibility for **1**.

Fig. 1 shows the molar magnetic susceptibility as a function of temperature, $\chi_M T$, for **1**. The effective magnetic moment, μ_{eff}, decreases with decreasing temperature down to the minimum of 1.87 μ_B at 42 K, and it increases abruptly up to the maximum of 3.85 μ_B at 26 K, then decreases again. This behavior is typical of ferrimagnetism. The effective moment at room temperature is 5.60 μ_B. The spin-only magnetic moment is 7.68 μ_B for the combination of Fe^{III} ($S = 5/2$) and Fe^{II} ($S = 2$). On the other hand, that is 5.19 μ_B for the combination of Fe^{III} ($S = 1/2$) and Fe^{II} ($S = 2$). Therefore, the effective magnetic moment of **1** is situated in the middle value between the magnetic moment for the high-spin and the low-spin states of Fe^{III}. This implies the possibility that the spin state of Fe^{III} is the spin equilibrium of the high-spin ($S = 5/2$) and the low-spin ($S = 1/2$) states. The inverse magnetic susceptibility as a function of temperature is shown in the inset of Fig. 1. From the fitting of inverse magnetic susceptibility with the Curie–Weiss low, $\chi = C/(T-\theta)$, Weiss temperature, θ, is estimated at −93 K. In order to confirm the ferrimagnetic phase-transition, FCM, ZFCM and RM were investigated. This result is shown in Fig. 2. From the analysis of magnetization curves, the ferrimagnetic transition temperature is estimated at 38 K. The magnetic property of **1** is similar to that of (*n*-C_4H_9)$_4$N[$Fe^{II}Fe^{III}$(ox)$_3$] which shows the ferrimagnetic phase-transition at $T_N = 43$ K [11].

Fig. 3 shows the ^{57}Fe Mössbauer spectra of **2** and **3** at 200 and 77 K, respectively. The Mössbauer parameters are summarized in Table 1. In both of the ^{57}Fe Mössbauer spectra of **2** and **3**, the spectra clearly indicates the presence of two quadrupole doublets,

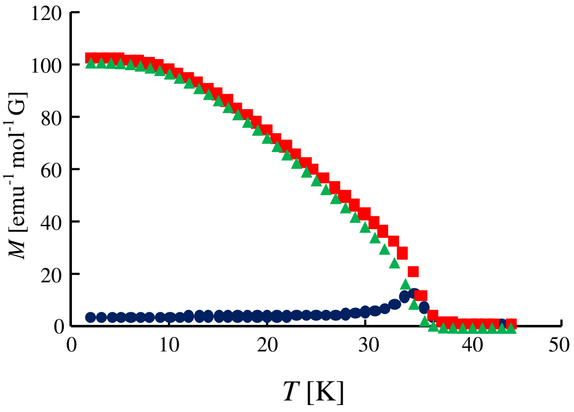

Fig. 2. Temperature dependence of magnetization for **1**. ■: Field cooled magnetization, ▲: remnant magnetization, ●: zero field cooled magnetization.